

Implications of the binary coalescence events found in O1 and O2 for the stochastic background of gravitational events

Nelson Christensen

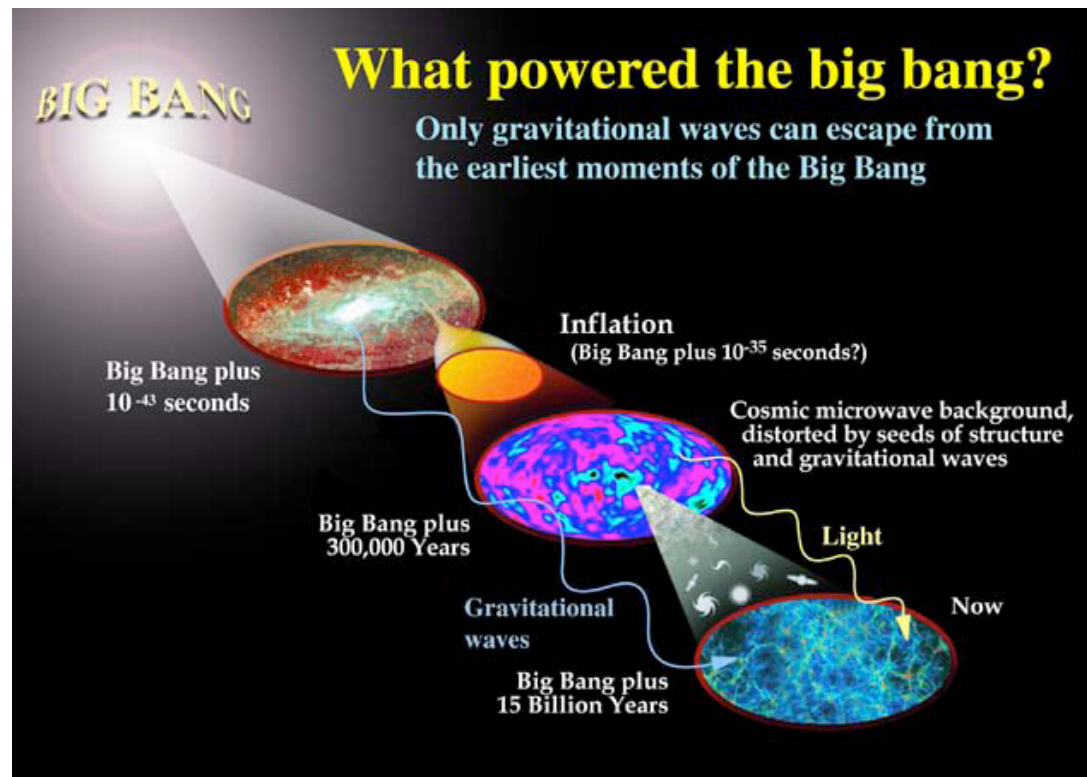
Artemis, Observatoire de la Côte d'Azur, Nice, France

Talk Outline

- Review of Advanced LIGO – Advanced Virgo Observing Runs 1 and 2 Observations
- Implications of the LIGO - Virgo detections on the background from BBHs
- LIGO-Virgo data analysis methods for a stochastic gravitational wave background
- O1 – O2 stochastic analysis and preliminary results
- Non-standard GR stochastic searches
- Future Advanced LIGO – Advanced Virgo Observing Runs, O3 Update
- Conclusions

Stochastic Gravitational-wave Background

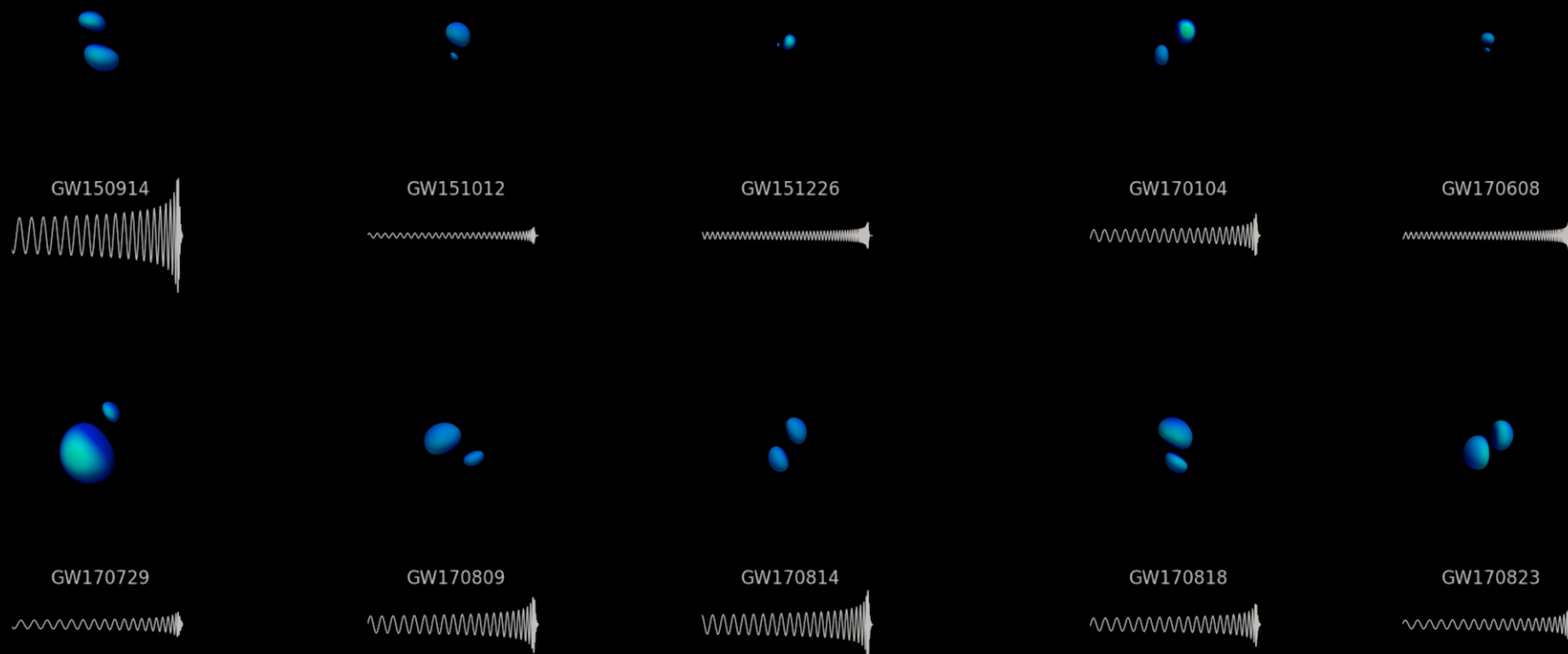
- Incoherent superposition of many unresolved sources.
- Cosmological:
 - » Inflationary epoch, preheating, reheating
 - » Phase transitions
 - » Cosmic strings
 - » Alternative cosmologies
- Astrophysical:
 - » Supernovae
 - » Magnetars
 - » Binary black holes
 - » Binary neutron stars
- Potentially could probe physics of the very-early Universe.



$$\Omega_{GW}(f) = \frac{f}{\rho_c} \frac{d\rho_{GW}}{df} \quad \Omega_{GW}(f) = A(f/f_{ref})^\alpha$$

O1 + O2 Binary Black Hole Events

LIGO/Virgo release first catalog of gravitational-wave events

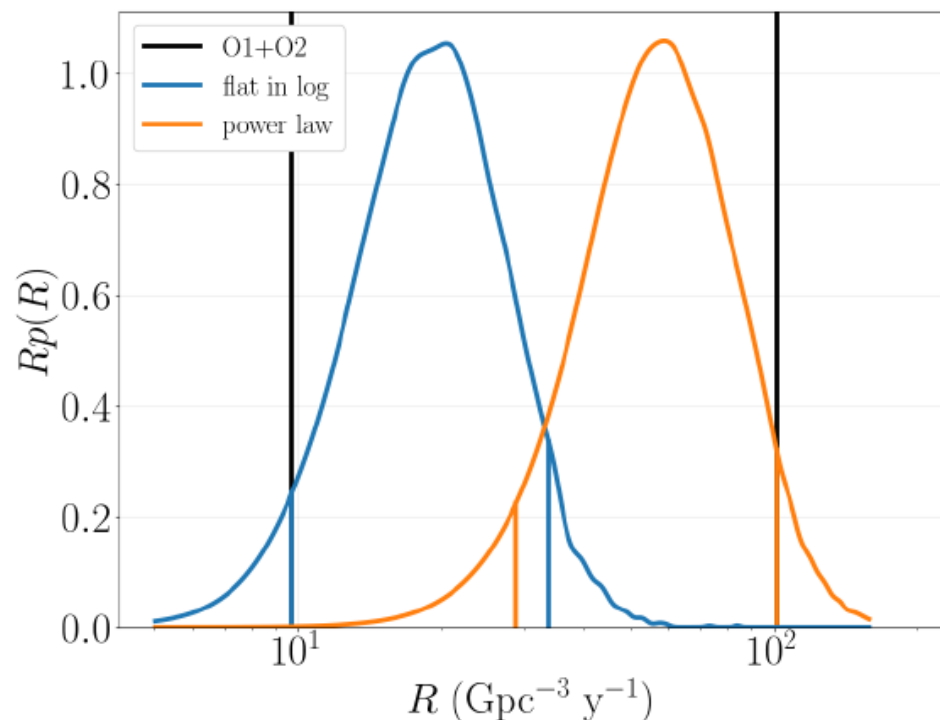


GWTC-1: A Gravitational-Wave Transient Catalog of Compact Binary Mergers Observed by LIGO and Virgo during the First and Second Observing Runs, [arXiv:1811.12907](https://arxiv.org/abs/1811.12907)

Implications of LIGO-Virgo detections

- LIGO and Virgo have detected 10 gravitational wave (GW) signals from binary black hole (BBH) mergers and 1 from a binary neutron star (BNS) merger.
- Besides the detection of loud individual sources at close distances, we expect to see the background formed by all the sources from the whole Universe (up to $z \sim 20$)
- The BBH observations have told us that black hole masses ($m_{1,2} \sim 8 - 51 M_{\odot}$) can be larger than previously expected.
- Revised previous predictions of the GW background from BBHs, assuming various formation scenarios.
- See “ GWTC-1: A Gravitational-Wave Transient Catalog of Compact Binary Mergers Observed by LIGO and Virgo during the First and Second Observing Runs“, arXiv: 1811.12907

Binary Black Hole Merger Rate

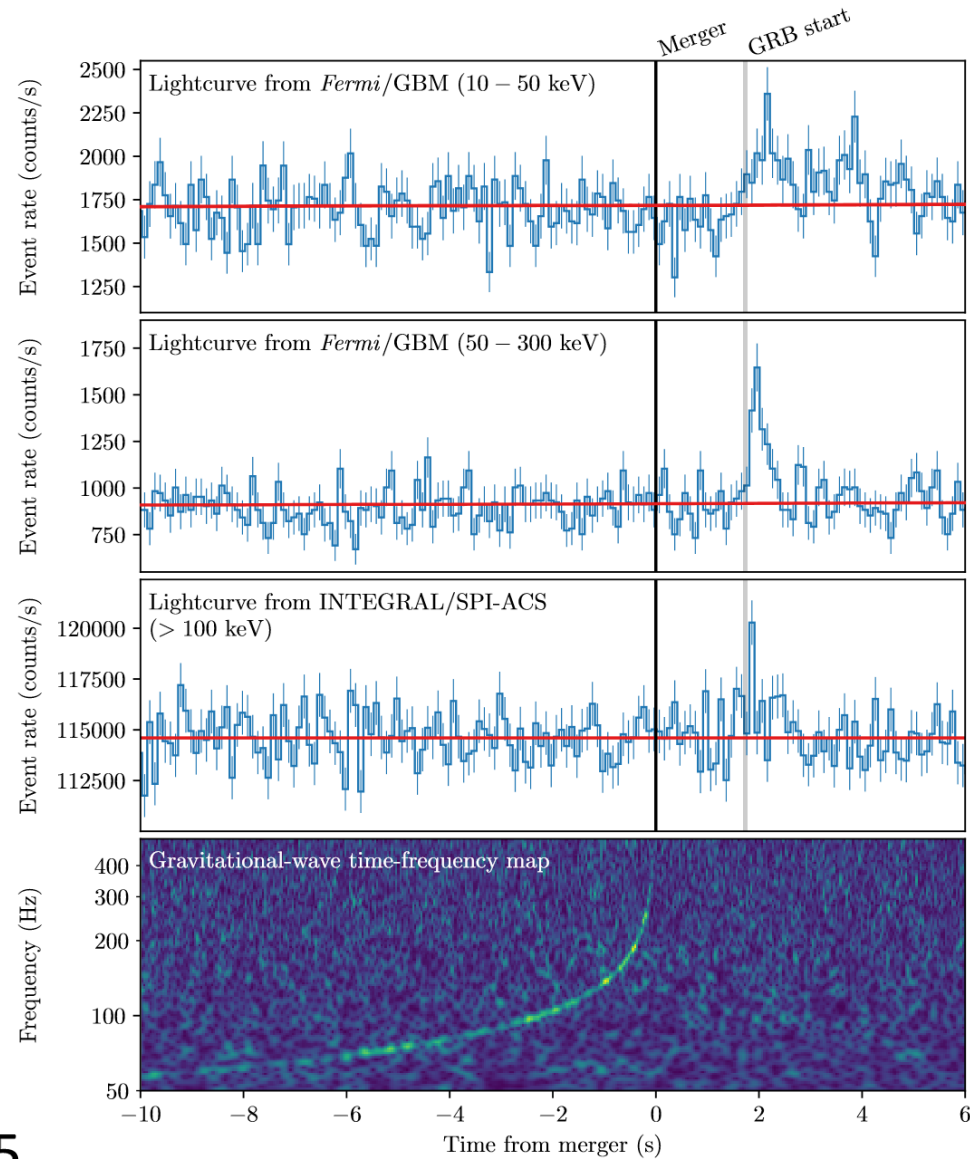


Merger Rate of $9.7\text{--}101 \text{ Gpc}^{-3}\text{yr}^{-1}$
for binary black holes assuming
fixed population distributions

FIG. 12. This figure shows the posterior distribution — combined from the results of PyCBC and GstLAL— on the BBH event rate for the flat in log (blue) and power-law (orange) mass distributions. The symmetric 90% confidence intervals are indicated with vertical lines beneath the posterior distribution. The union of intervals is indicated in black.

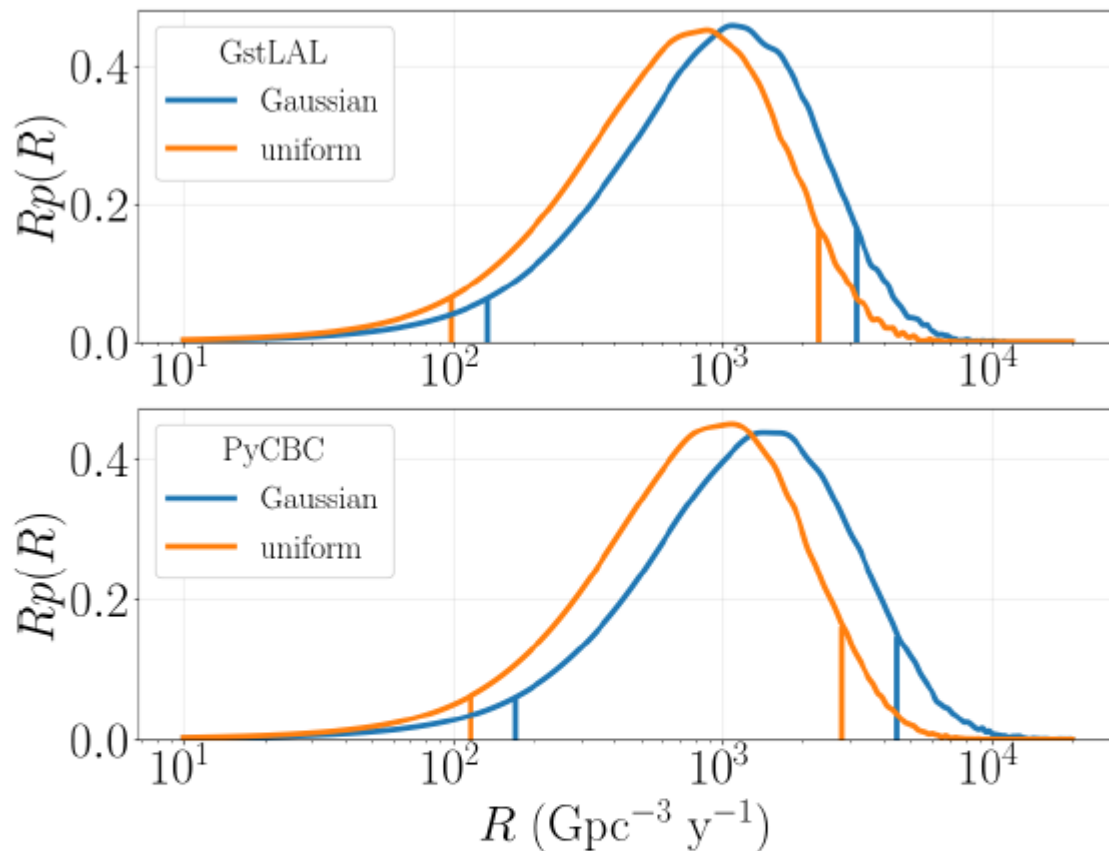
GRB 170817A and GW170817

- A gravitational wave event 1.7 s before gamma ray observation
- Binary neutron star merger at 40 Mpc
- Start of gravitational-wave multimessenger astronomy.



$$\Delta t = 1.74 \pm 0.05$$

Binary Neutron Star Merger Rate



Merger Rate of 110–3840 $\text{Gpc}^{-3} \text{yr}^{-1}$ for binary neutron stars assuming fixed population distributions.

Upper limit of neutron star - black hole merger rate 90% upper limit of $610 \text{Gpc}^{-3} \text{yr}^{-1}$.

FIG. 13. This figure shows the posterior distributions of the BNS event rate for the GstLAL and PyCBC searches. The uniform mass distribution corresponds to the orange curves and Gaussian mass distributions corresponds to the blue curves. The symmetric 90% confidence intervals are indicated with vertical lines beneath the posterior distributions.

Astrophysics: Binary Formation

- Two binary formation mechanisms have been proposed.
- Field:
 - » Starting from a binary star system, with each star going through the core-collapse to a black hole.
- Dynamic:
 - » Individually formed black holes in dense environments (globular clusters) fall toward the center of the potential well, where they dynamically form binaries (and are often ejected).

Primordial black holes are also another hot area of research and discussion. See, for example:
arXiv:1603.00464, arXiv:1608.06699 and an interesting LIGO-Virgo limit on sub-solar mass BBHs arXiv:1808.04771, 1904.08976

Implications for a Stochastic Background of GWs

- For every detected binary merger, there are many more that are too distant and too faint.
- They generate a stochastic background of gravitational waves.

$$\Omega_{\text{GW}}(f; \theta_k) = \frac{f}{\rho_c H_0} \int_0^{z_{\text{max}}} dz \frac{R_m(z, \theta_k) \frac{dE_{\text{GW}}}{df_s}(f_s, \theta_k)}{(1+z)E(\Omega_M, \Omega_\Lambda, z)}$$

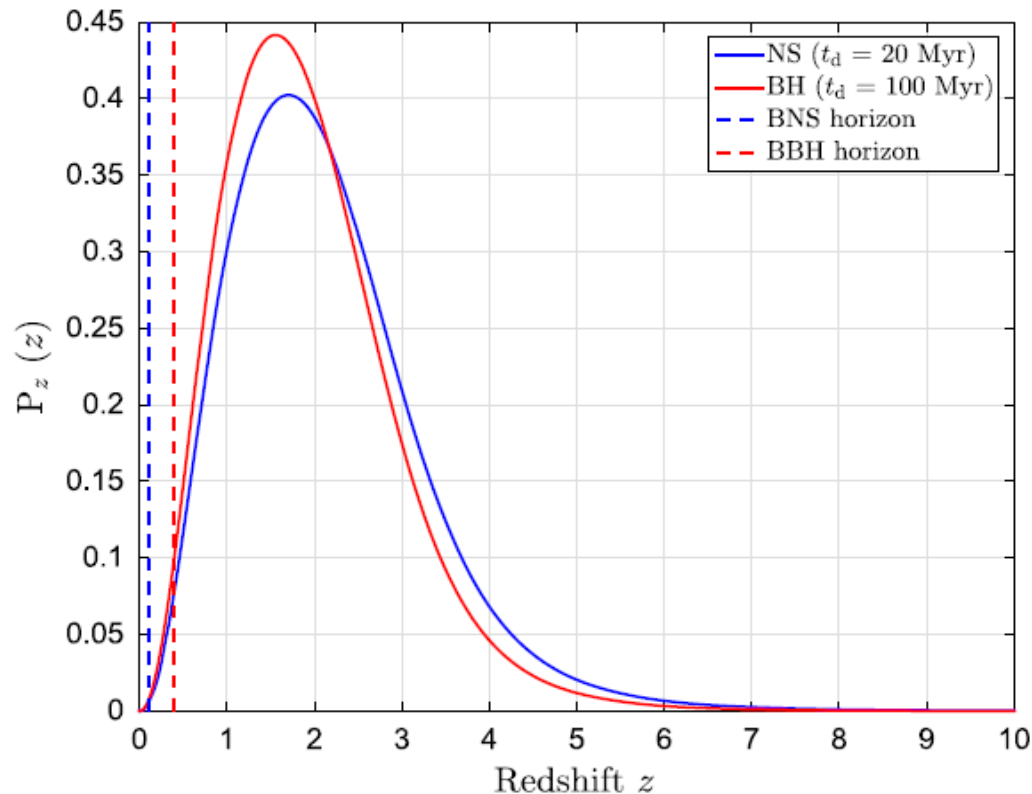
Merger Rate
Source Energy Spectrum

↑
Cosmology

- Relatively high rate and large masses of observed systems implies a relatively strong stochastic background.

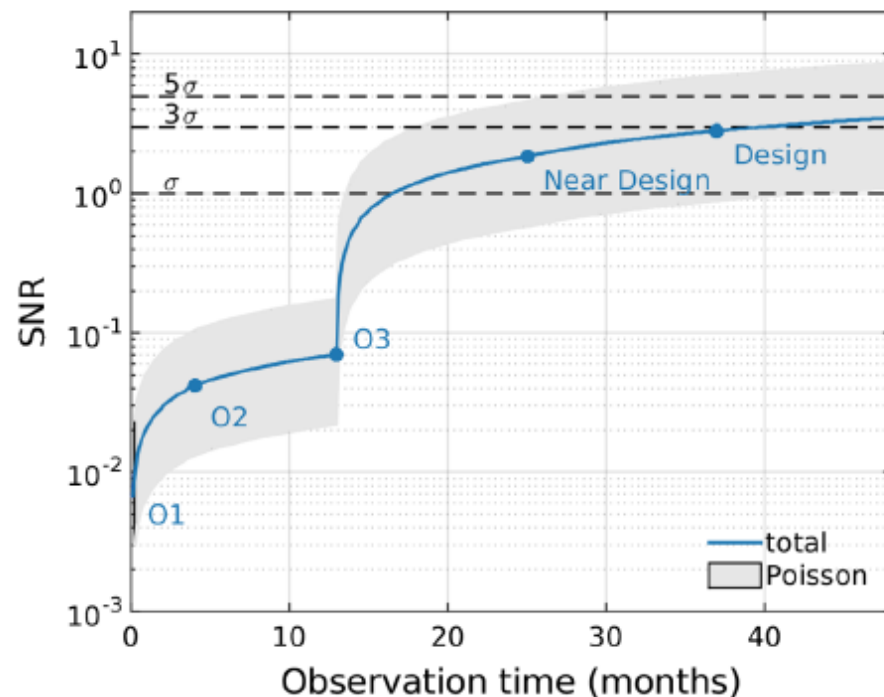
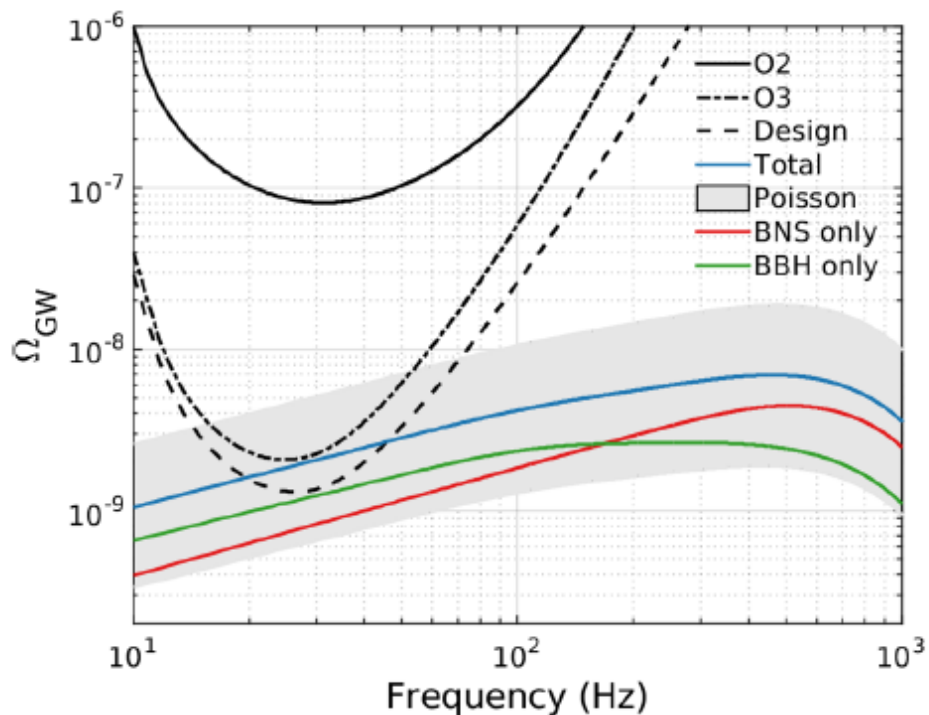
Implications for a Stochastic Background of GWs

Probing compact binary decays predominantly between $z \sim 1 - 3$.



Source redshift probability distribution for binary neutron stars and (blue) and binary black holes (red).

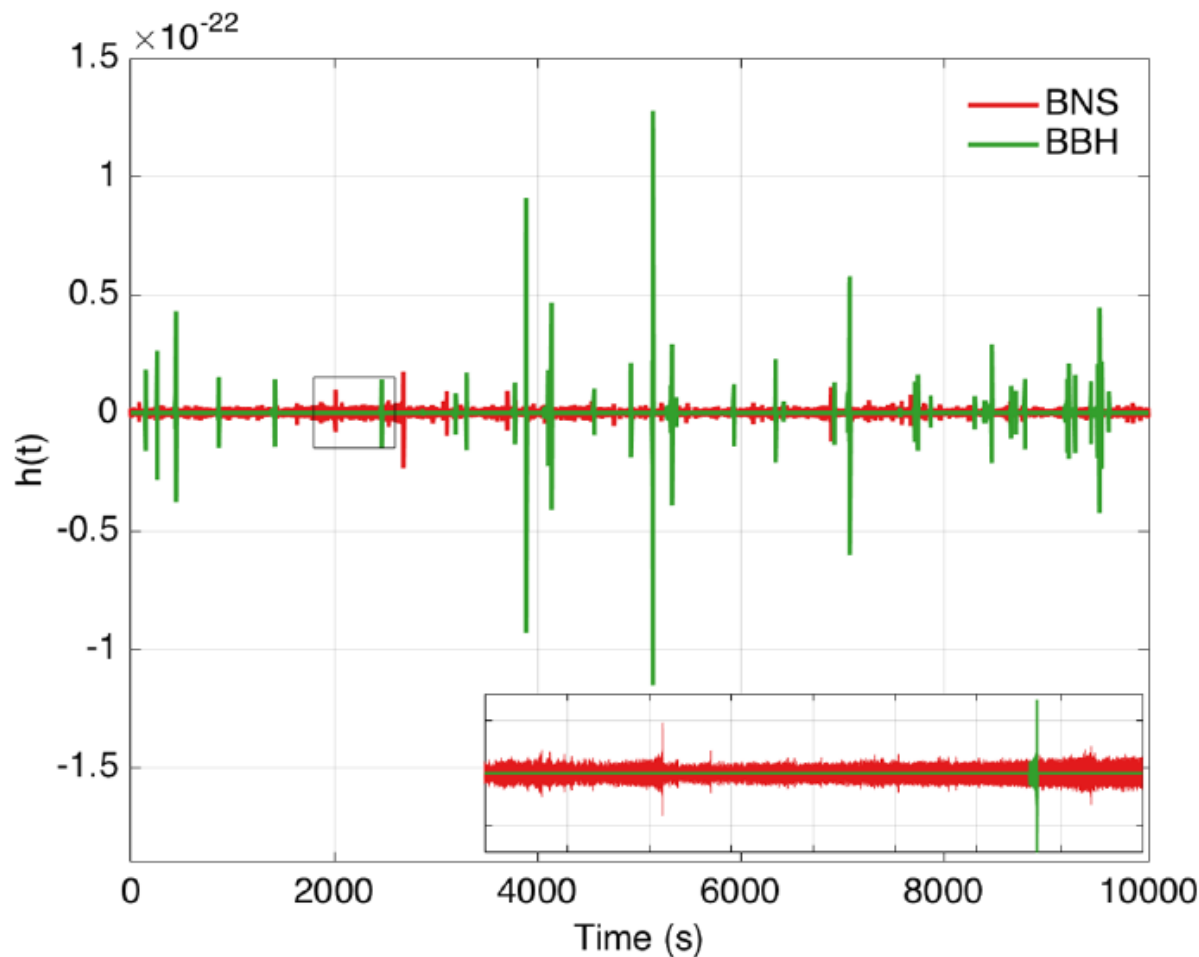
Implications for a Stochastic Background of GWs



Based on the Field formation mechanism

Assumptions are necessary; best information available in literature.

Implications for a Stochastic Background of GWs

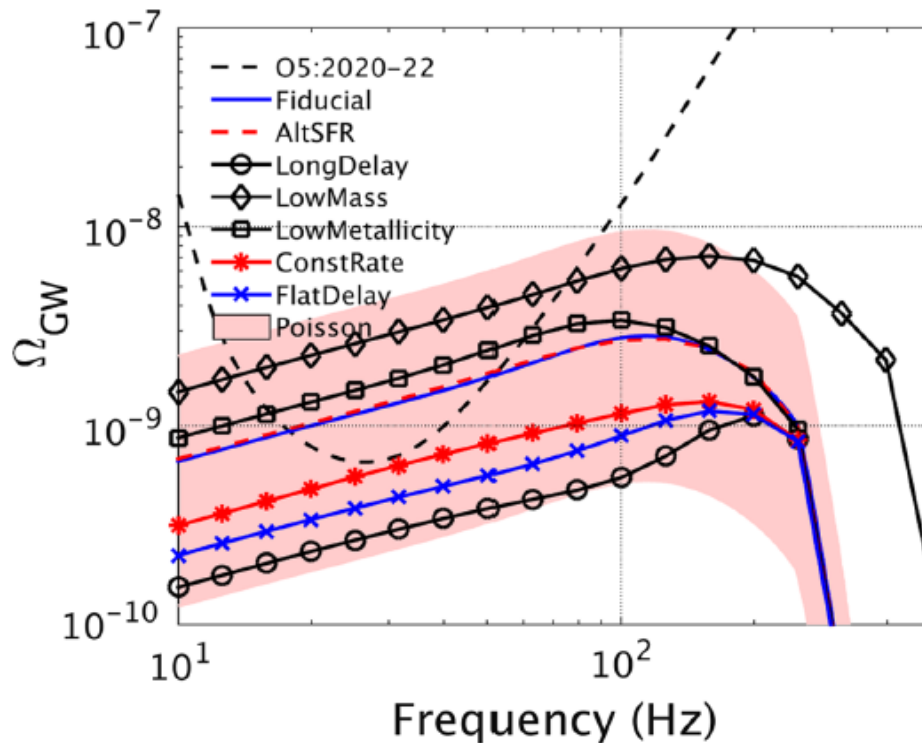


Simulated time series illustrating the character of the BBH and BNS signals in the time domain.

Continuous BNS
Popcorn BBH

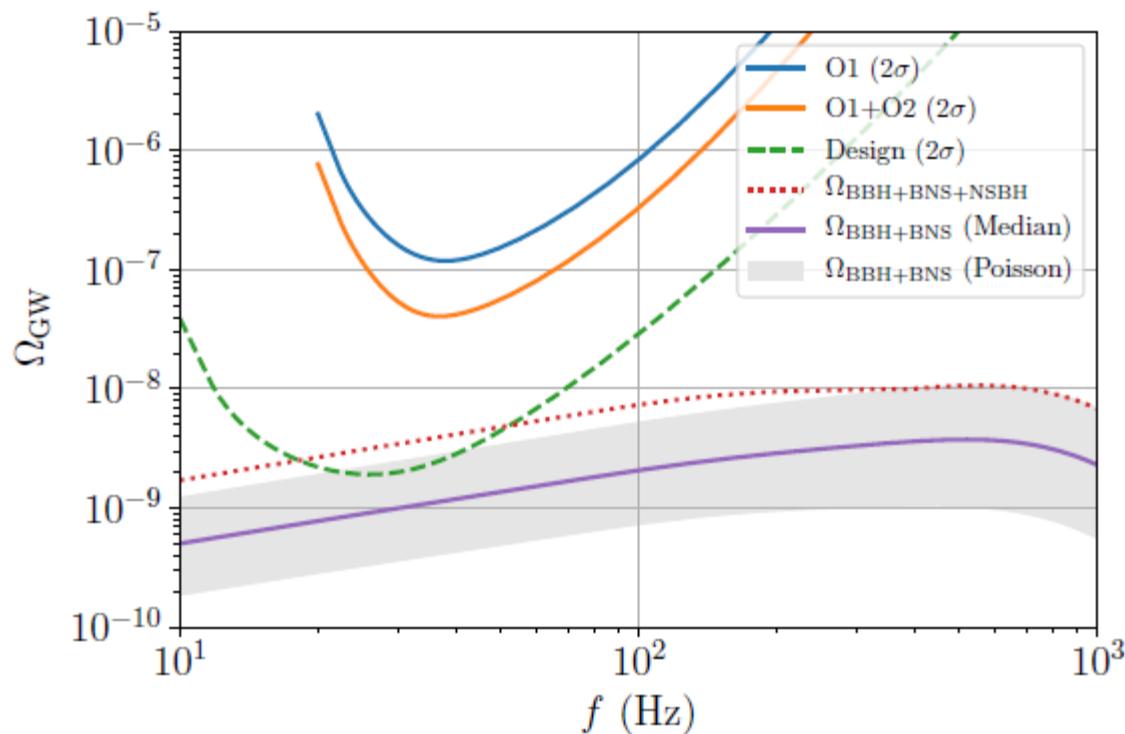
Even though the backgrounds have very different structure in the time domain, the energy in both backgrounds is comparable below 100 Hz.

Alternative Models



- Model variations imply relatively small changes in the energy spectrum.
- Large Poisson statistical uncertainty.
- Dominated by $z \sim 1-2$ contributions.
- Conservative estimates.
- A foreground to cosmological models of stochastic background.

Implications for a Stochastic Background of GWs



All of O1 + O2.

All observed events.

Mean value

$$\Omega_{\text{gw}}(25\text{Hz}) > 10^{-9}$$

Less uncertainty in stochastic background level

Less sensitive to CBC background than reported in GW170817 implications paper (PRL **120**, 091101, 2018) due to lower rate estimate and increased low freq noise (coating measurements)

ArXiv 1903.02886, Phys. Rev. D 100, 061101(R) (2019)

There is a very real probability that LIGO-Virgo will observe this BBH produced stochastic background in the next 5 years.

Gravitational wave background from Population III binary black holes consistent with cosmic reionization

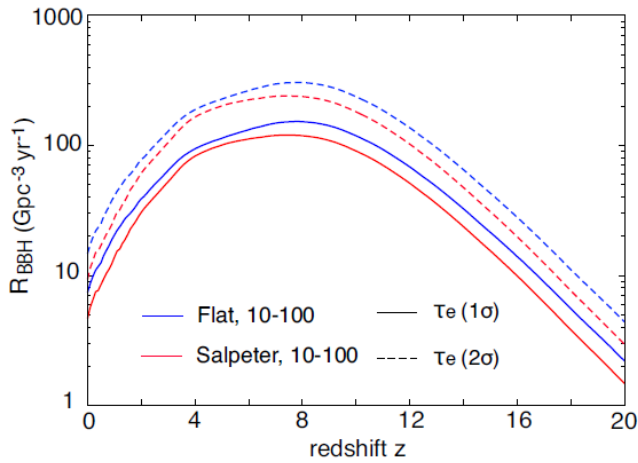


Figure 3. Merger rate of PopIII BBHs for different assumed IMFs, as in Fig. 2. The data is taken from K14, but renormalized to be consistent with the electrons scattering optical depth τ_e measured by *Planck* within the 1σ (solid) and 2σ (dashed) error (Eq. 1 with $f_{\text{esc,m}} = 0.1$ and $\eta_{\text{ion}} = 5 \times 10^4$).

Potentially a stronger stochastic background than what we would expect from direct BBH observations.

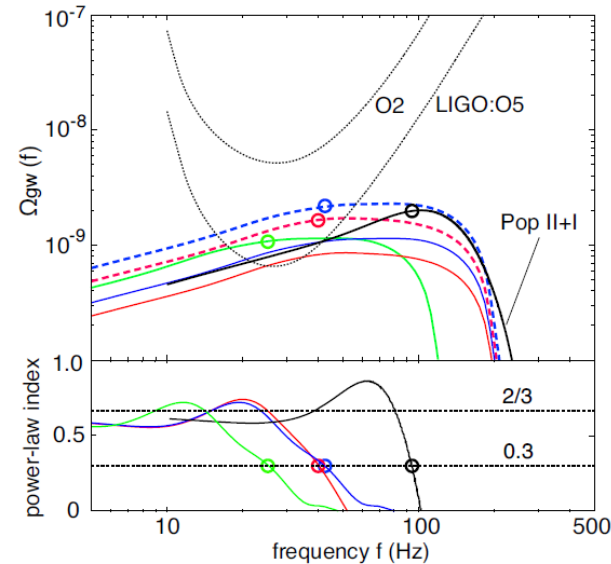


Figure 4. *Top*: spectra of GWB produced by PopIII BBHs for the same IMFs, $f_{\text{esc,m}}$ and τ_e as in Fig. 3 (blue and red curves). We assume binaries with the average chirp mass of $\langle M_{\text{chirp}} \rangle = 30 M_{\odot}$ on circular orbits. The background expected from all unresolved PopII+PopI BBHs is shown for reference (solid black curve, Abbott et al. 2016b, their fiducial model). Black dotted curves show the expected sensitivity of AdLIGO/Virgo in the observing runs O2 and O5. The green solid curve is the same as the blue solid curve, but with a higher chirp mass of $\langle M_{\text{chirp}} \rangle = 50 M_{\odot}$ and with a lower merging rate by a factor of $3/5$. *Bottom*: the spectral index; open circles mark the frequencies above which $\alpha < 0.3$.

Did LIGO Detect Dark Matter?

- “There remains a window for masses $20 M_{\odot} \lesssim M_{\text{bh}} \lesssim 100 M_{\odot}$ where primordial black holes (PBHs) may constitute the dark matter.”
- Reasonable rate estimates overlap LIGO rate limits.
- No neutrino or optical counterparts.
- “They may be distinguished from mergers of BHs from more traditional astrophysical sources through the observed mass spectrum, their high ellipticities, or their stochastic gravitational wave background.” S. Bird et al., PRL 116, 201301 (2016)
- “We show that if PBHs make up the dark matter, then roughly one event should have a detectable eccentricity given LIGO’s expected sensitivity and observing time of six years.” I. Cholis et al., PRD 94, 084013 (2016)

Stochastic Background – Primordial Black Hole

“We have shown that the amplitude of this spectrum is significantly lower than that arising from the stellar BBH mergers, although there is currently a large uncertainty in the local merger rate for stellar BBH systems.

...

Consequently, the stochastic GW background measurement with Advanced LIGO detectors is unlikely to detect this background.”

Other studies are more optimistic:

<https://arxiv.org/abs/1610.08725>
<https://arxiv.org/abs/1610.08479>
<https://arxiv.org/abs/1711.10458>
<https://arxiv.org/abs/1812.11011>

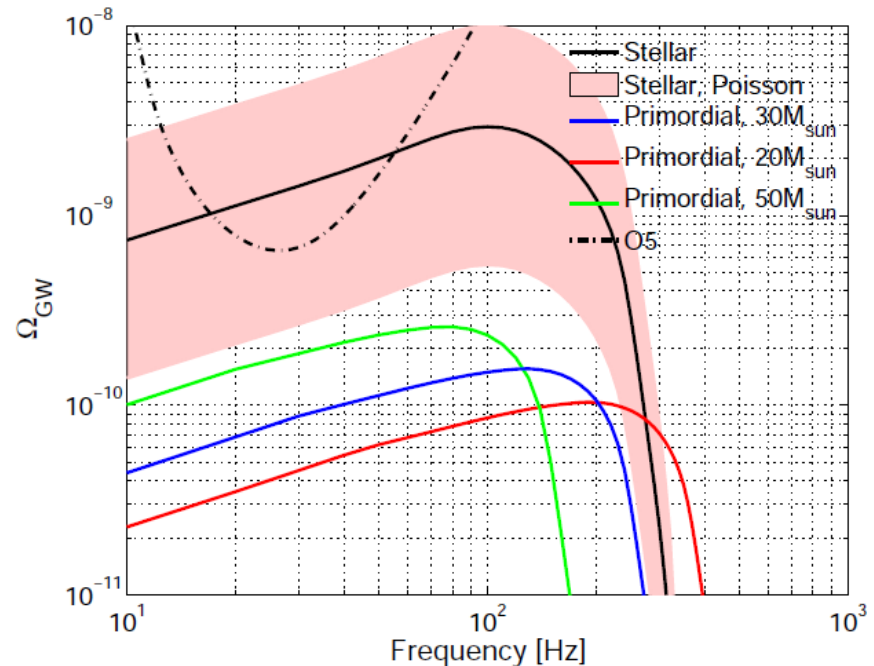


FIG. 4: Gravitational-wave energy density for the primordial BBH model is shown as a function of frequency for several values of the black hole mass, assuming the Ludlow et al. concentration model [28] and the Watson et al. model of the halo mass function [31]. Also shown is the projected final sensitivity of advanced detectors, denoted O5, as well as the fiducial stellar model and its Poisson error band [34].

Data Analysis

- Assume stationary, unpolarized, isotropic and Gaussian stochastic background
- Cross correlate the output of detector pairs to eliminate the noise

$$s_i = h_i + n_i$$

$$\langle s_1 s_2 \rangle = \langle h_1 h_2 \rangle + \underbrace{\langle n_1 n_2 \rangle}_0 + \underbrace{\langle h_1 n_2 \rangle}_0 + \underbrace{\langle n_1 h_2 \rangle}_0$$

Isotropic search

- Frequency domain cross product:

$$Y = \int \tilde{s}_1^*(f) \tilde{Q}(f) \tilde{s}_2(f) df$$

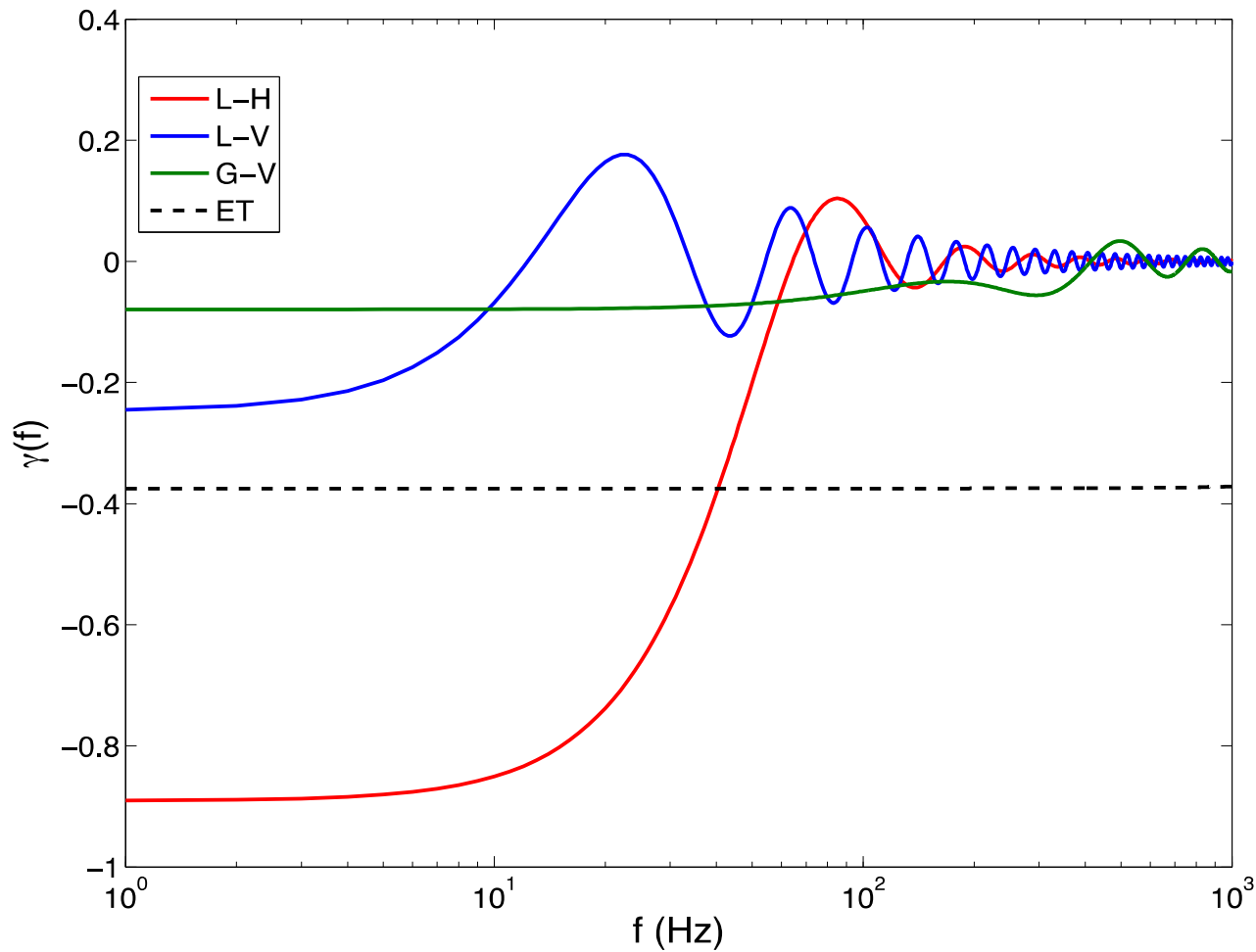
- optimal filter:

$$\tilde{Q}(f) \propto \frac{\gamma(f) \Omega_{gw}(f)}{f^3 P_1(f) P_2(f)} \text{ with } \Omega_{gw}(f) \equiv \Omega_\alpha f^\alpha$$

- in the limit noise \gg GW signal

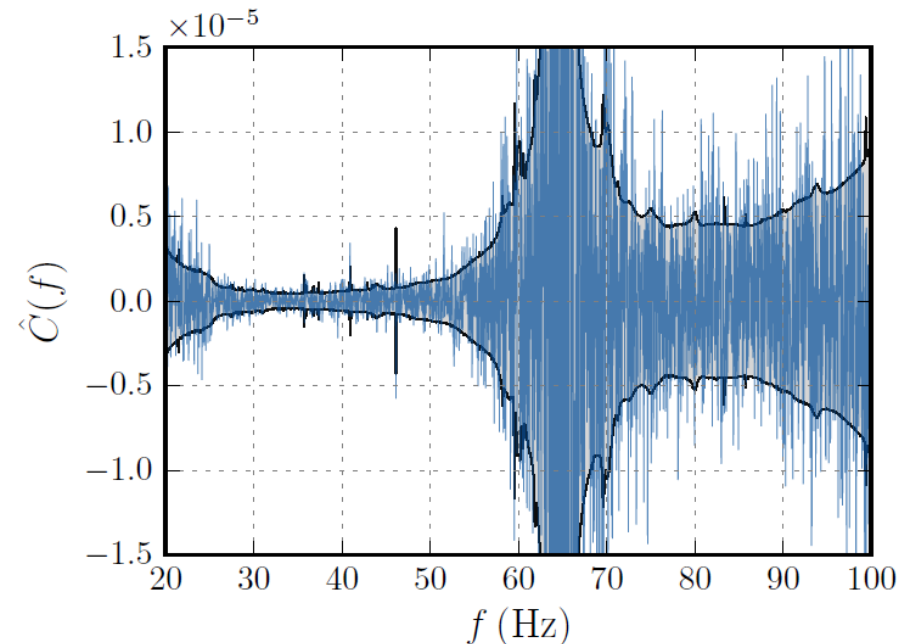
$$\text{Mean}(Y) = \Omega_0 T, \text{ Var}(Y) \equiv \sigma^2 \mu T, \text{ SNR } \mu \sqrt{T}$$

Overlap reduction function



O1+O2 Stochastic Search Results

- No evidence for a stochastic background for both the isotropic and direction searches
- Put upper limits on the energy density for different power indices
- For $\alpha=0$, the isotropic bound is 2.8x better than the O1 result
- $\Omega_{\text{gw}}(25\text{Hz}) < 6.0 \times 10^{-8}$



The cross-correlation spectrum between Advanced LIGO's Hanford and Livingston detectors during O2.

Arxiv:1903:02886

α	Uniform prior		Log-uniform prior	
	O1+O2	O1	O1+O2	O1
0	6.0×10^{-8}	1.7×10^{-7}	3.5×10^{-8}	6.4×10^{-8}
2/3	4.8×10^{-8}	1.3×10^{-7}	3.0×10^{-8}	5.1×10^{-8}
3	7.9×10^{-9}	1.7×10^{-8}	5.1×10^{-9}	6.7×10^{-9}
Marg.	1.1×10^{-7}	2.5×10^{-7}	3.4×10^{-8}	5.5×10^{-8}

TABLE II. 95% credible upper limits on Ω_{ref} for different power law models (fixed α), as well as marginalizing over α , for combined O1 and O2 data (current limits) and for O1 data (previous limits) [66]. We show results for two priors, one which is uniform in Ω_{ref} , and one which is uniform in the logarithm of Ω_{ref} .

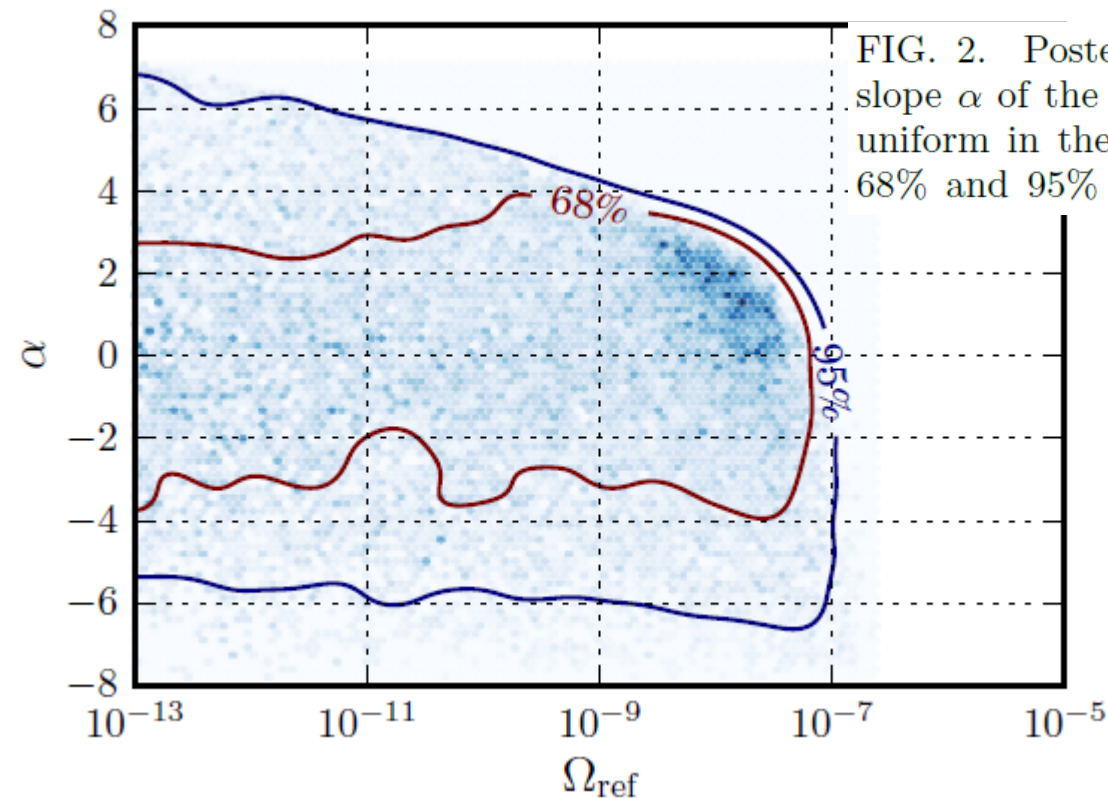


FIG. 2. Posterior distribution for the amplitude Ω_{ref} and slope α of the stochastic background, using a prior which is uniform in the logarithm of Ω_{ref} , along with contours with 68% and 95% confidence-level, using combined O1 and O2

Note LIGO S1 results PRD **69**,
122004 (2004)

$$\Omega_0 \sim 50$$

An improvement of 9 orders of
magnitude in 15 years.

Test of General Relativity with the Stochastic Gravitational-wave Background

A new search. Using Advanced LIGO O1, O2 (and future) data to search for 6 polarizations. Non-GR. New search pipeline. Theoretical work on-going in parallel.

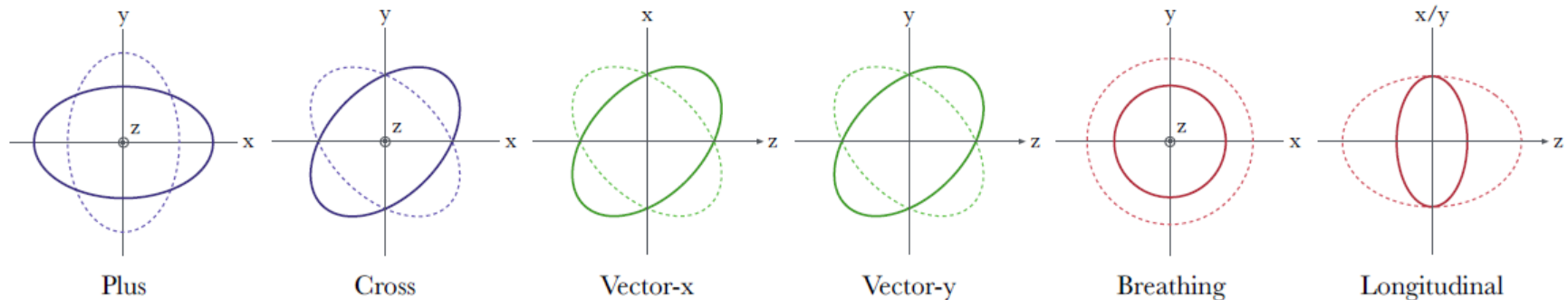


FIG. 1. Deformation of a ring of test particles under the six gravitational wave polarizations allowed in general metric theories of gravity. Each wave is assumed to propagate in the z -direction. While General Relativity allows only for two tensor polarizations (Plus and Cross), alternate theories allow for two vector (X and Y) and/or two scalar (Breathing and Longitudinal) polarization modes.

Test of General Relativity with the Stochastic Gravitational-wave Background

Results for a search for scalar, vector and tensor polarizations with O1-O2 data.

A fully Bayesian (nested sampling) parameter estimation method will assign upper limits for energy of the different polarizations. Constraints will be placed on various non-GR theories.

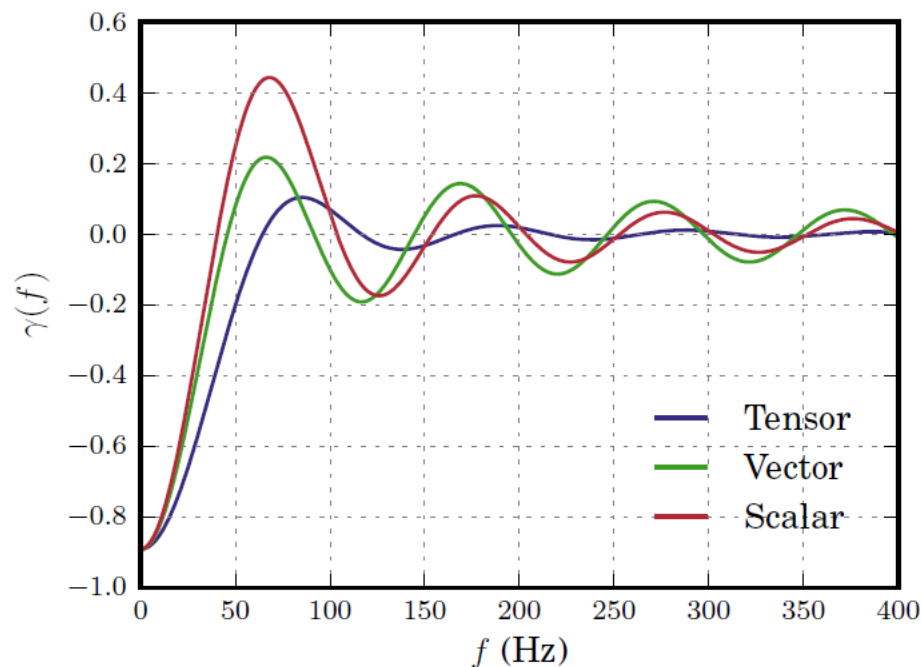


FIG. 2. Overlap reduction functions quantifying Advanced LIGO's sensitivity to isotropic backgrounds of tensor, vector, and scalar-polarized gravitational wave backgrounds.

Test of General Relativity

O1-O2 isotropic analysis - non-GR modes

- allow contributions from all polarization modes:

$$\langle \hat{C}(f) \rangle_{\text{TVS}} = \beta_T(f) \Omega_{\text{ref}}^T \left(\frac{f}{f_{\text{ref}}} \right)^{\alpha_T} + \beta_V(f) \Omega_{\text{ref}}^V \left(\frac{f}{f_{\text{ref}}} \right)^{\alpha_V} + \beta_S(f) \Omega_{\text{ref}}^S \left(\frac{f}{f_{\text{ref}}} \right)^{\alpha_S}$$

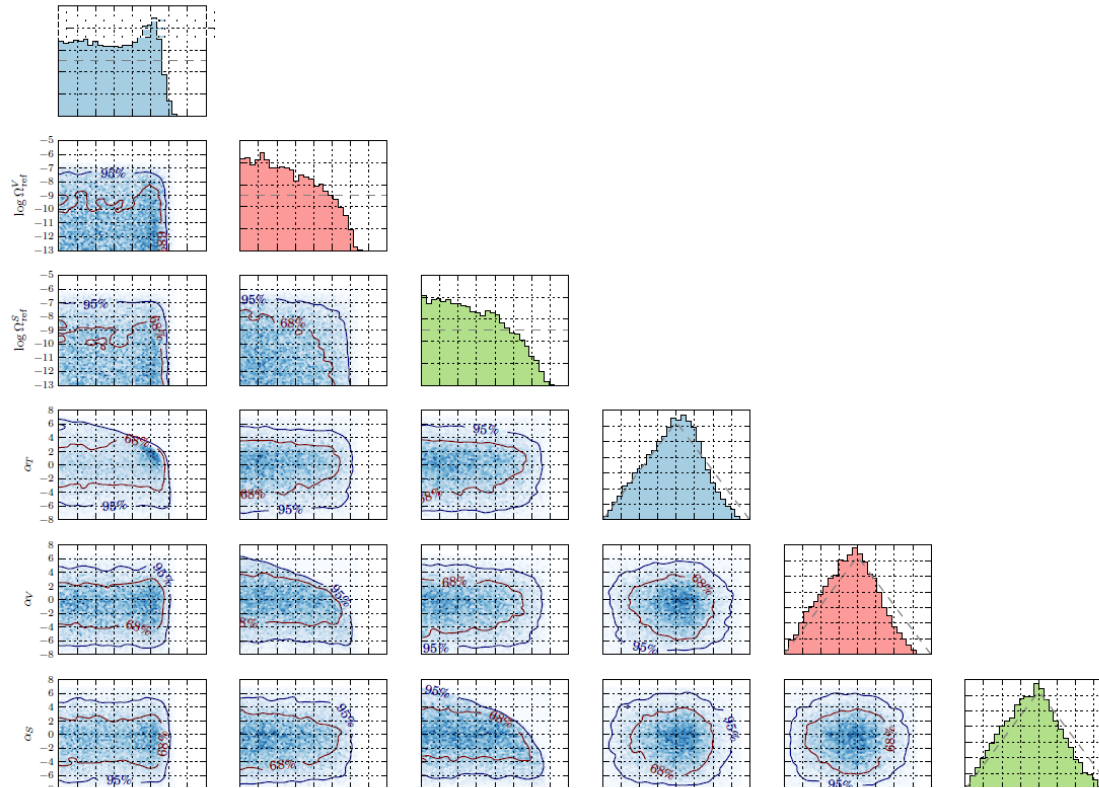
where $\beta_A(f) \equiv \frac{\gamma_A(f)}{\gamma_T(f)}$, $A = \{T, V, S\}$

- log bayes factors consistent with gaussian noise and GR-polarization modes
- set ULs assuming all three modes potentially present, marginalizing over amplitudes and spectral indices for all but one mode

Polarization	Uniform prior	Log-uniform prior
Tensor	8.2×10^{-8}	3.2×10^{-8}
Vector	1.2×10^{-7}	2.9×10^{-8}
Scalar	4.2×10^{-7}	6.1×10^{-8}

Arxiv:1903:02886

Test of General Relativity



Arxiv:1903:02886

Hypothesis	$\Omega_{\text{ref}}^{T,95\%}$	$\Omega_{\text{ref}}^{V,95\%}$	$\Omega_{\text{ref}}^{S,95\%}$	α_T	α_V	α_S
V	-	3.3×10^{-8}	-	-	$-0.8^{+5.4}_{-5.7}$	-
S	-	-	7.0×10^{-8}	-	-	$-0.7^{+5.8}_{-5.8}$
TV	3.3×10^{-8}	3.0×10^{-8}	-	$-0.2^{+5.3}_{-6.1}$	$-0.9^{+5.4}_{-5.6}$	-
TS	3.4×10^{-8}	-	6.2×10^{-8}	$-0.2^{+5.3}_{-6.2}$	-	$-0.8^{+5.8}_{-5.7}$
VS	-	3.2×10^{-8}	6.4×10^{-8}	-	$-0.9^{+5.5}_{-5.6}$	$-0.8^{+5.9}_{-5.7}$
TVS	3.2×10^{-8}	2.9×10^{-8}	6.1×10^{-8}	$-0.2^{+5.3}_{-6.1}$	$-0.8^{+5.4}_{-5.7}$	$-0.8^{+5.8}_{-5.7}$

Directional searches

- Relax assumption of isotropy and generalize the search for a stochastic signal to the case of arbitrary angular distribution.

$$\Omega_{\text{GW}}(f) \equiv \frac{f}{\rho_c} \frac{d\rho_{\text{GW}}}{df} = \frac{2\pi^2}{3H_0^2} f^3 H(f) \int_{S^2} d\hat{\Omega} \mathcal{P}(\hat{\Omega})$$

$$\mathcal{P}(\hat{\Omega}) = \mathcal{P}_\alpha \mathbf{e}_\alpha(\hat{\Omega})$$

Radiometer Analysis

Spherical Harmonic
Decomposition

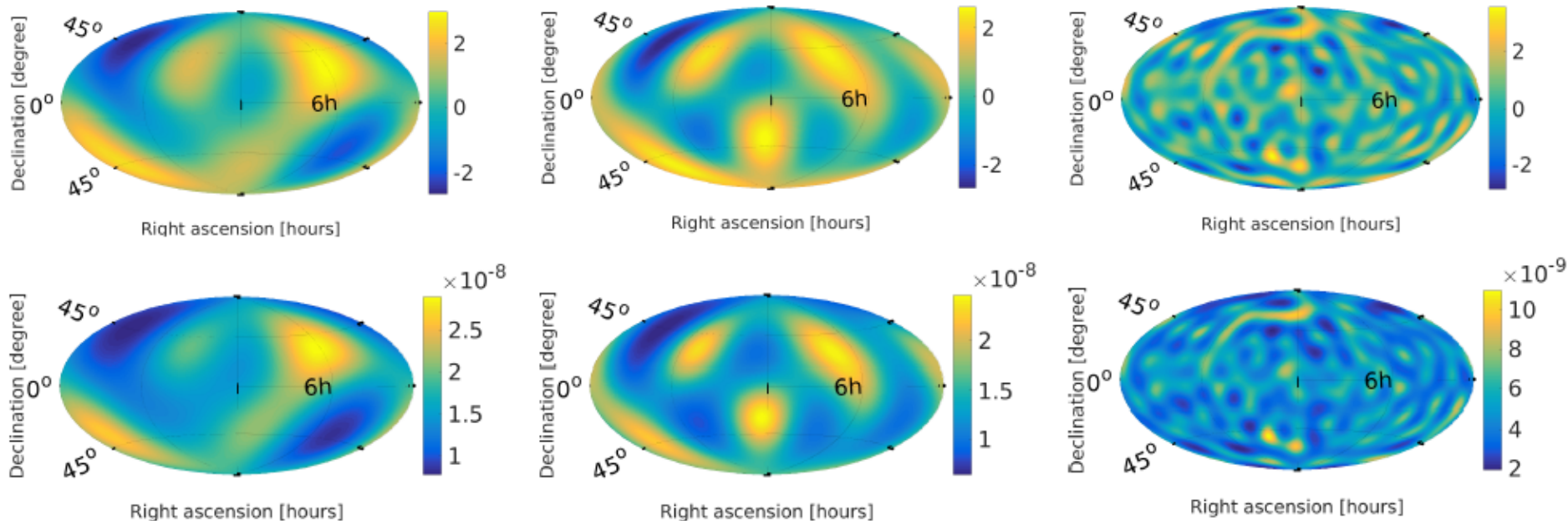
$$\mathcal{P}(\hat{\Omega}) \equiv \eta(\hat{\Omega}_0) \delta^2(\hat{\Omega}, \hat{\Omega}_0)$$

$$\mathcal{P}(\hat{\Omega}) \equiv \sum_{lm} \mathcal{P}_{lm} Y_{lm}(\hat{\Omega})$$

O1-O2 Directional – Extended Sources

Spherical Harmonic Decomposition (SHD)

2-3 times better than O1 only result



All-sky (broadband) Results

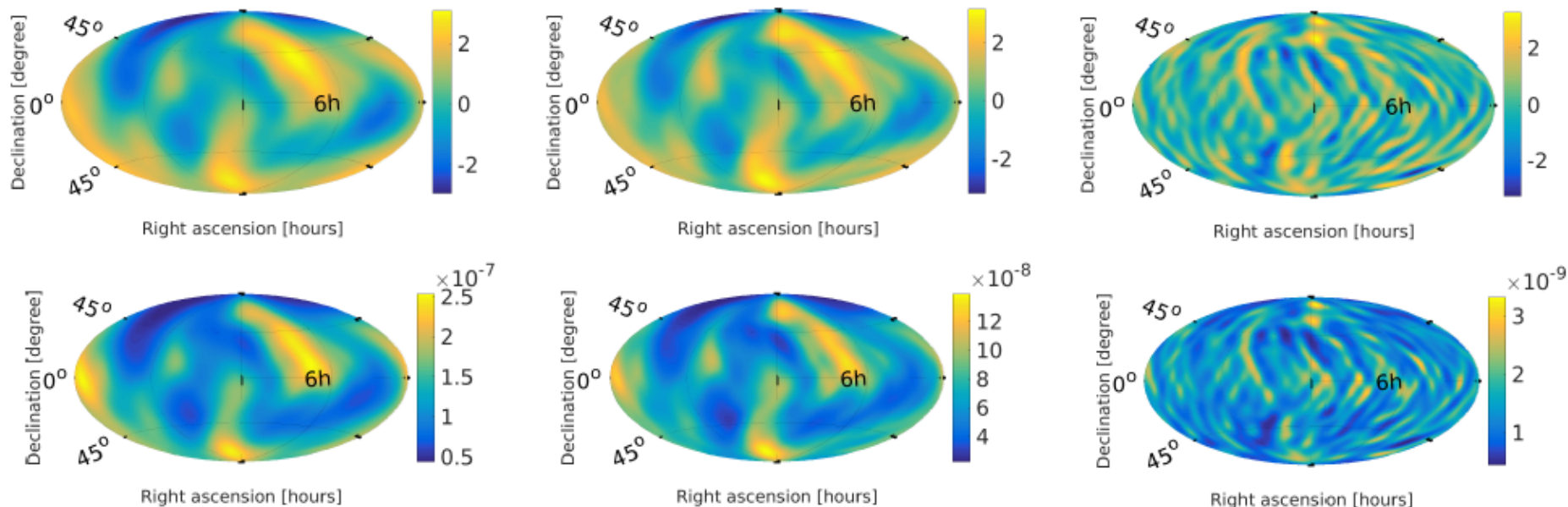
α	Ω_{gw}	$H(f)$	Max SNR (% p -value)		Upper limit ranges		O1 Upper limit ranges	
			BBR	SHD	BBR ($\times 10^{-8}$)	SHD ($\times 10^{-8}$)	BBR ($\times 10^{-8}$)	SHD ($\times 10^{-8}$)
0	constant	$\propto f^{-3}$	3.09 (9)	2.98 (9)	4.4 – 25	0.78 – 2.90	15 – 65	3.2 – 8.7
2/3	$\propto f^{2/3}$	$\propto f^{-7/3}$	3.09 (20)	2.61 (31)	2.3 – 14	0.64 – 2.47	7.9 – 39	2.5 – 6.7
3	$\propto f^3$	constant	3.27 (66)	3.57 (27)	0.05 – 0.33	0.19 – 1.1	0.14 – 1.1	0.5 – 3.1

Upper Limit maps [$\Omega_{\text{gw}} \text{ sr}^{-1}$]

Arxiv:1903:08844, Phys. Rev. D 100, 062001 (2019)

O1 Directional – Point Sources

2-3 times better than O1 only result



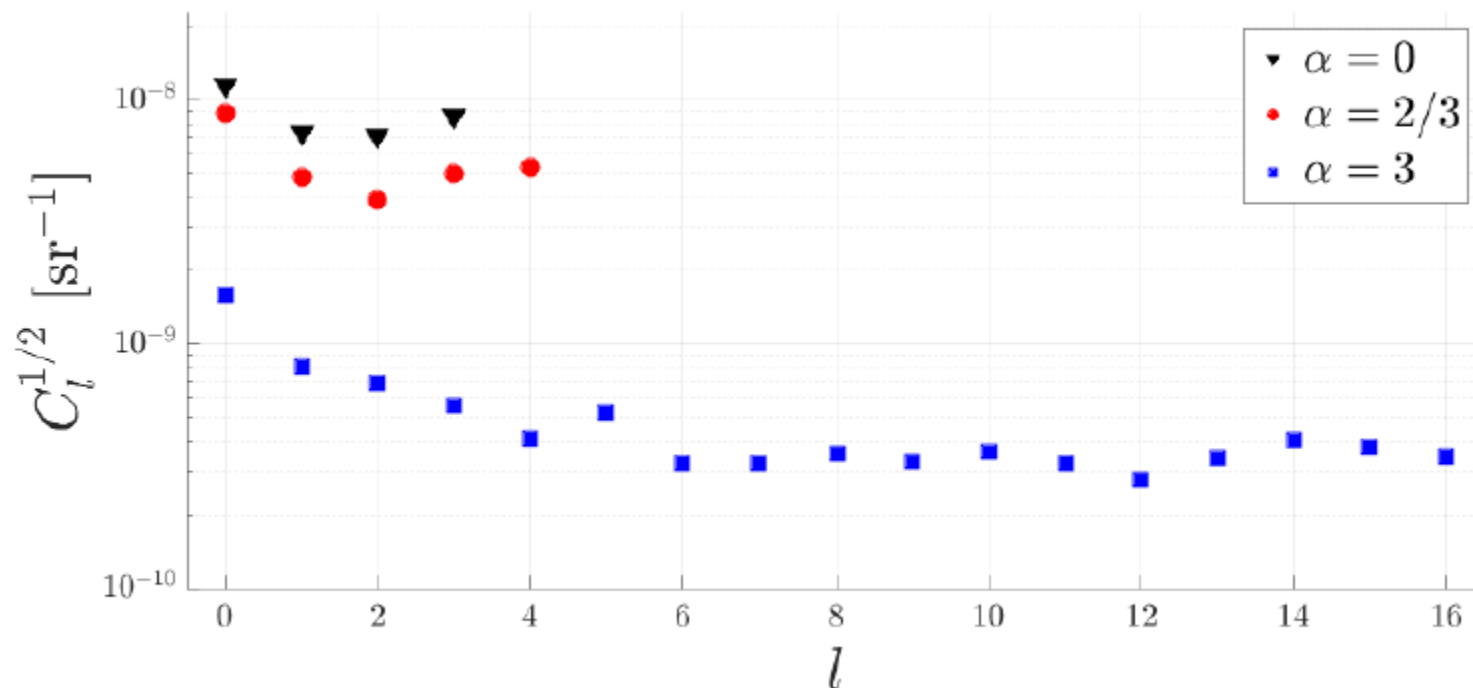
All-sky (broadband) Results

α	Ω_{gw}	$H(f)$	Max SNR (% p -value)		Upper limit ranges		O1 Upper limit ranges	
			BBR	SHD	BBR ($\times 10^{-8}$)	SHD ($\times 10^{-8}$)	BBR ($\times 10^{-8}$)	SHD ($\times 10^{-8}$)
0	constant	$\propto f^{-3}$	3.09 (9)	2.98 (9)	4.4 – 25	0.78 – 2.90	15 – 65	3.2 – 8.7
2/3	$\propto f^{2/3}$	$\propto f^{-7/3}$	3.09 (20)	2.61 (31)	2.3 – 14	0.64 – 2.47	7.9 – 39	2.5 – 6.7
3	$\propto f^3$	constant	3.27 (66)	3.57 (27)	0.05 – 0.33	0.19 – 1.1	0.14 – 1.1	0.5 – 3.1

Upper Limit maps [$\text{erg cm}^{-2} \text{s}^{-2} \text{Hz}^{-1}$]

Arxiv:1903:08844

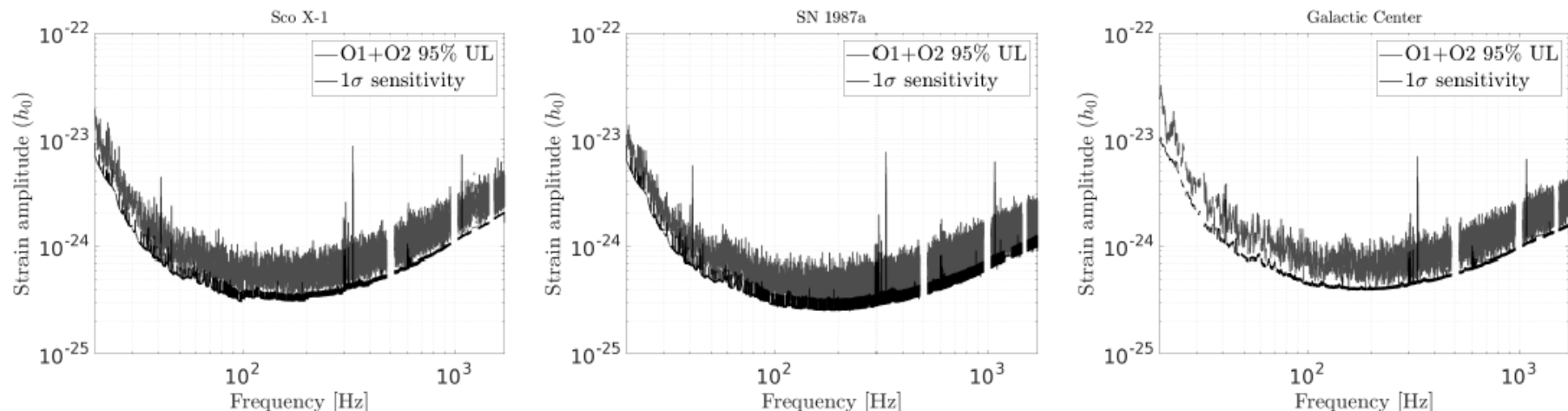
O1-O2 Directional Analysis - Angular Power Spectra



Upper limits on C_l 's at 95% confidence for the SHD analyses.

Upper limits are a factor of 2.5-3 better than for O1, and several orders of magnitude greater than theoretical predictions for CBCs and cosmic strings

O1-O2 Directional – Directed Narrowband Radiometer



Narrowband Radiometer Results

Direction	Max SNR	p -value (%)	Frequency (Hz) (± 0.016 Hz)	Best UL ($\times 10^{-25}$)	Frequency band (Hz)
Sco X-1	4.80	4.5	1602.09	4.2	183.6 – 184.6
SN 1987A	4.95	1.7	181.81	3.6	247.75 – 248.75
Galactic Center	3.80	98	20.28	4.7	156.8 – 157.8

Best strain upper limits are a factor 1.5 better than O1,
 $h_0 < 3.6 - 4.7 \times 10^{-25}$

Correlated Magnetic Noise from the Schumann Resonances

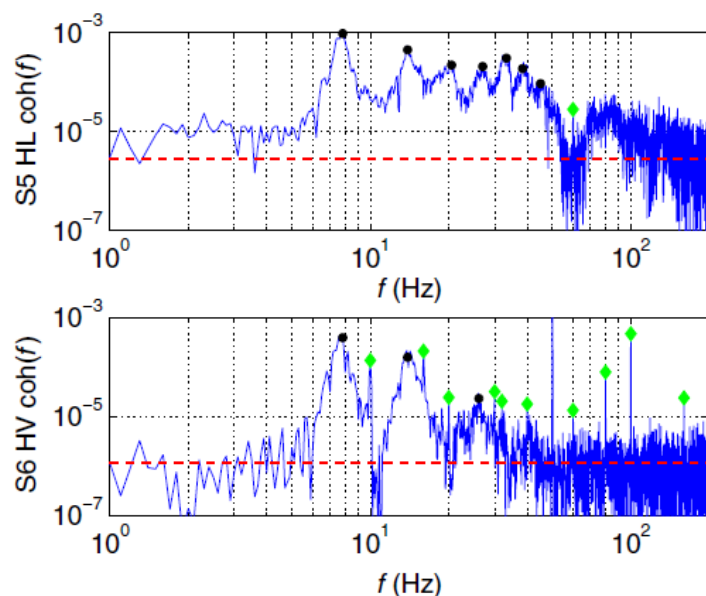


FIG. 1 (color online). Magnetometer coherence spectra for LHO-LLO during the LIGO S5 science run (top, $t_{\text{obs}} = 330$ dy) and for LHO-Virgo during S6-VSR2/3 (bottom, $t_{\text{obs}} = 100$ dy). Schumann resonance peaks are indicated with black circles while electronic noise lines are indicated with green diamonds. The red dashed line indicates the average value expected for uncorrelated noise. Some LHO-LLO peaks are obscured by 60 Hz electronic noise. The frequency resolution is 0.1 Hz.

Monitor correlated magnetic noise level.
PRD **87**, 123009 (2013)

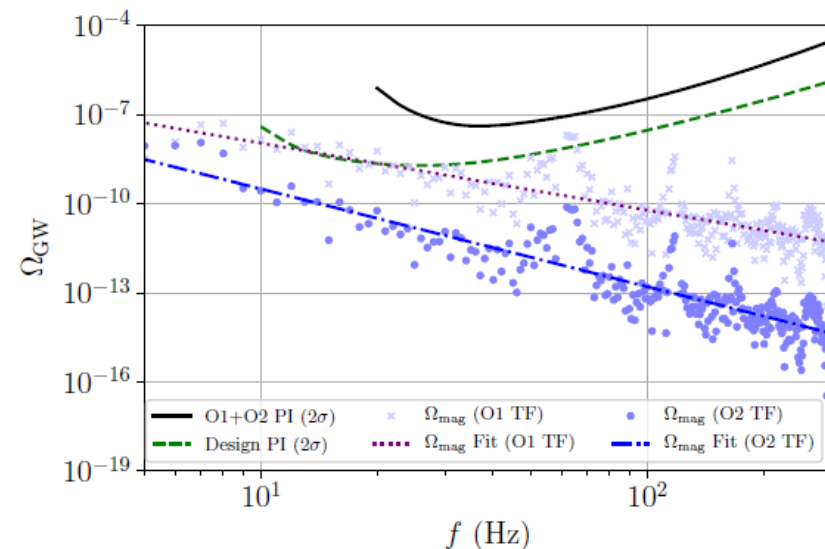
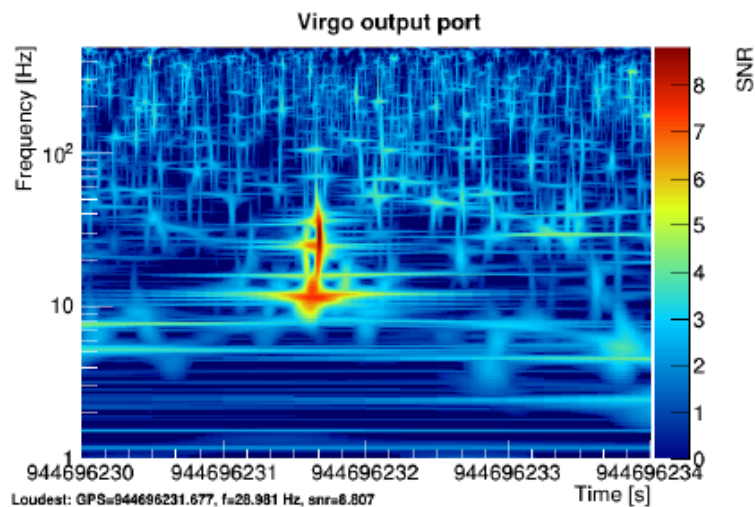
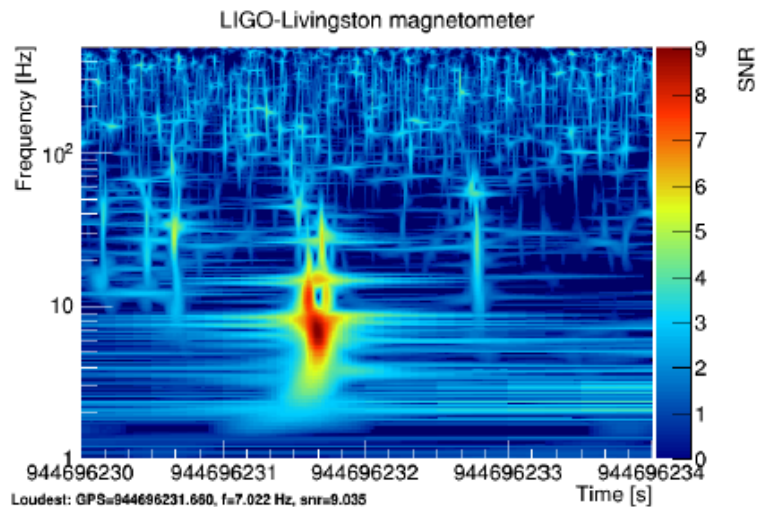
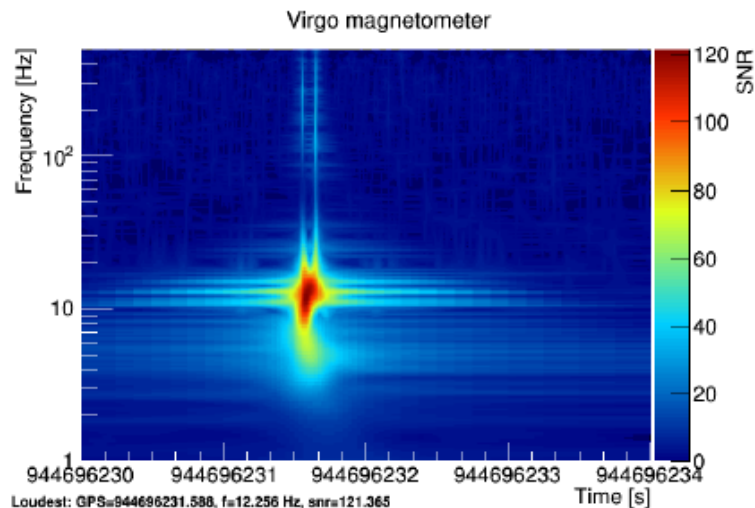
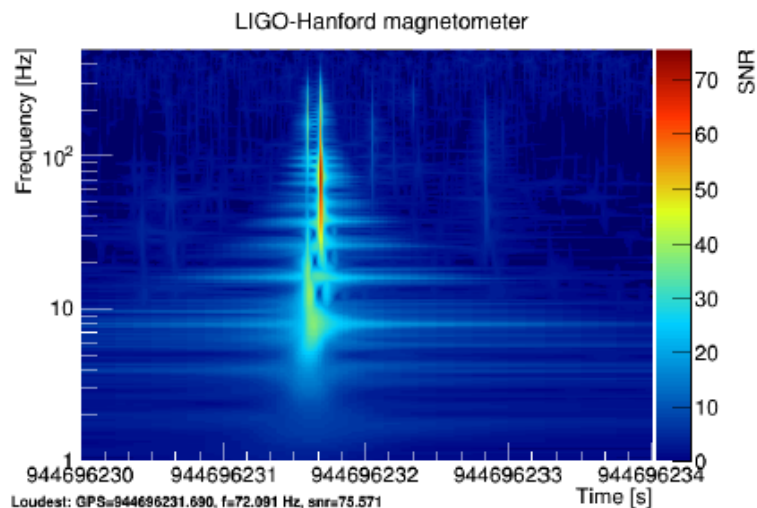


FIG. 4. Conservative estimate of correlated magnetic noise. We assume a conservative transfer function (TF) based on measurements as described in the text. The first Schumann resonance at 8 Hz is visible, higher harmonics are below the noise floor. There is a zero of the overlap function at 64 Hz which leads to an apparent feature in Ω_{mag} . Power line harmonics have been removed, as in the cross-correlation analysis. The two trend lines show power law fits to the magnetometer spectra, scaled by the O1 (purple dotted) and end-of-O2 (blue dot-dashed) transfer functions. This demonstrates the effect of reducing the magnetic coupling in O2. The trend for the noise budget lies well below the solid black O2 PI curve, which indicates that correlated magnetic noise is negligible in O2. However magnetic contamination may be an issue in future observing runs.

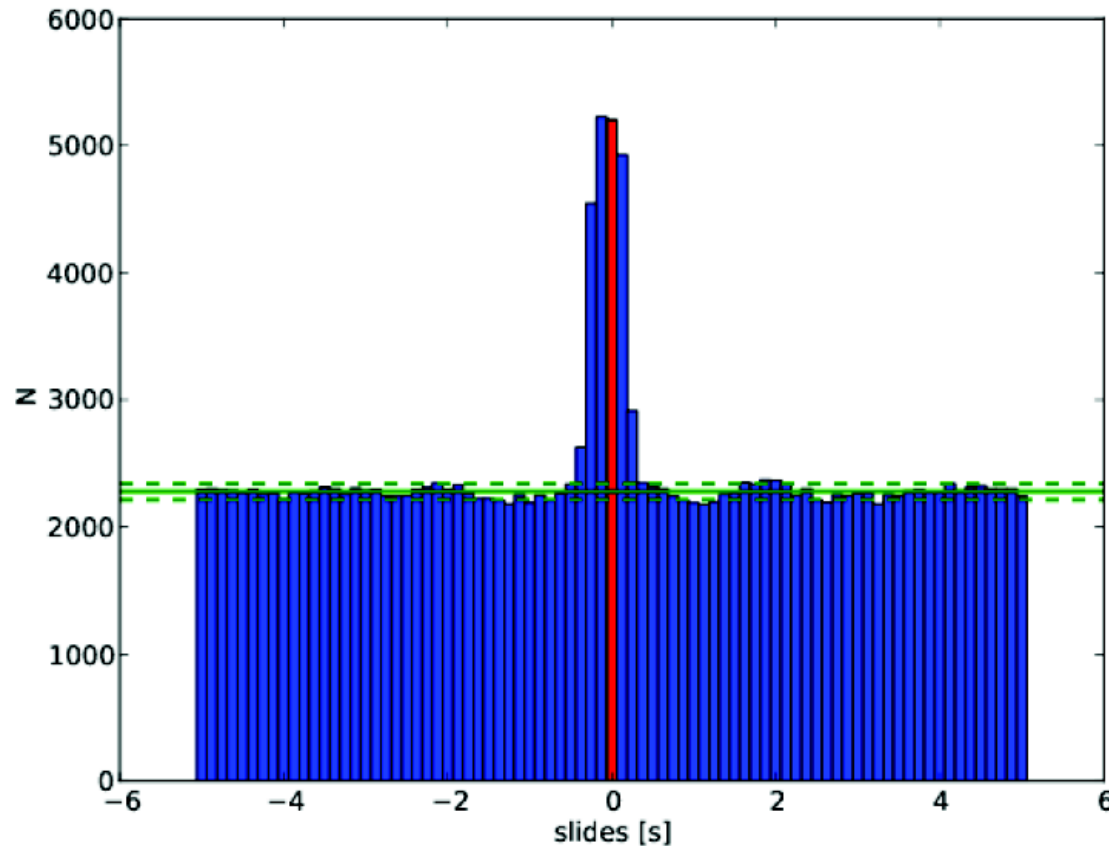
Arxiv:1903:02886

Correlated Transient Magnetic Noise – The Source of the Schumann Resonances



Time-frequency spectrograms of magnetometers located at the LIGO-Hanford, Virgo and LIGO-Livingston at the time of the December 12, 2009 positive Gigantic Jet at 23:36:56.55 UTC. The signal is clearly present in the magnetometers. Bottom right spectrogram shows the event in the Virgo gravitational-wave strain, $h(t)$, data.

Correlated Transient Magnetic Noise – Time Slide Study For Coincident Events



The number of coincident triggers as a function of time delay for magnetometers located at LIGO-Hanford and Virgo. The horizontal line represents the mean value of the time slide results (excluding the 0.625 s covered by the central 5 bins), while the dashed lines represent the standard deviation (again excluding the central 5 bins).

Constraints on Cosmic String Parameters from Stochastic and Burst Search Results

O2 results: *1903:02886*

$G\mu/c^2 < 1.1 \times 10^{-6}$ for
M=1 (large loop
distribution PRD **73**,
105001 (2006))

$G\mu/c^2 < 2.1 \times 10^{-14}$ for
M=3 (Large loop
Nambu-Goto
distribution of Ringeval
et al. JCAP **1010**, 003
(2010))

Note from pulsar timing

$G\mu/c^2 < 1.6 \times 10^{-11}$

and

$G\mu/c^2 < 6.2 \times 10^{-12}$

respectively PRX **6**,
011035 (2016)

CONSTRAINTS ON COSMIC STRINGS USING DATA FROM ...

PHYS. REV. D **97**, 102002 (2018)

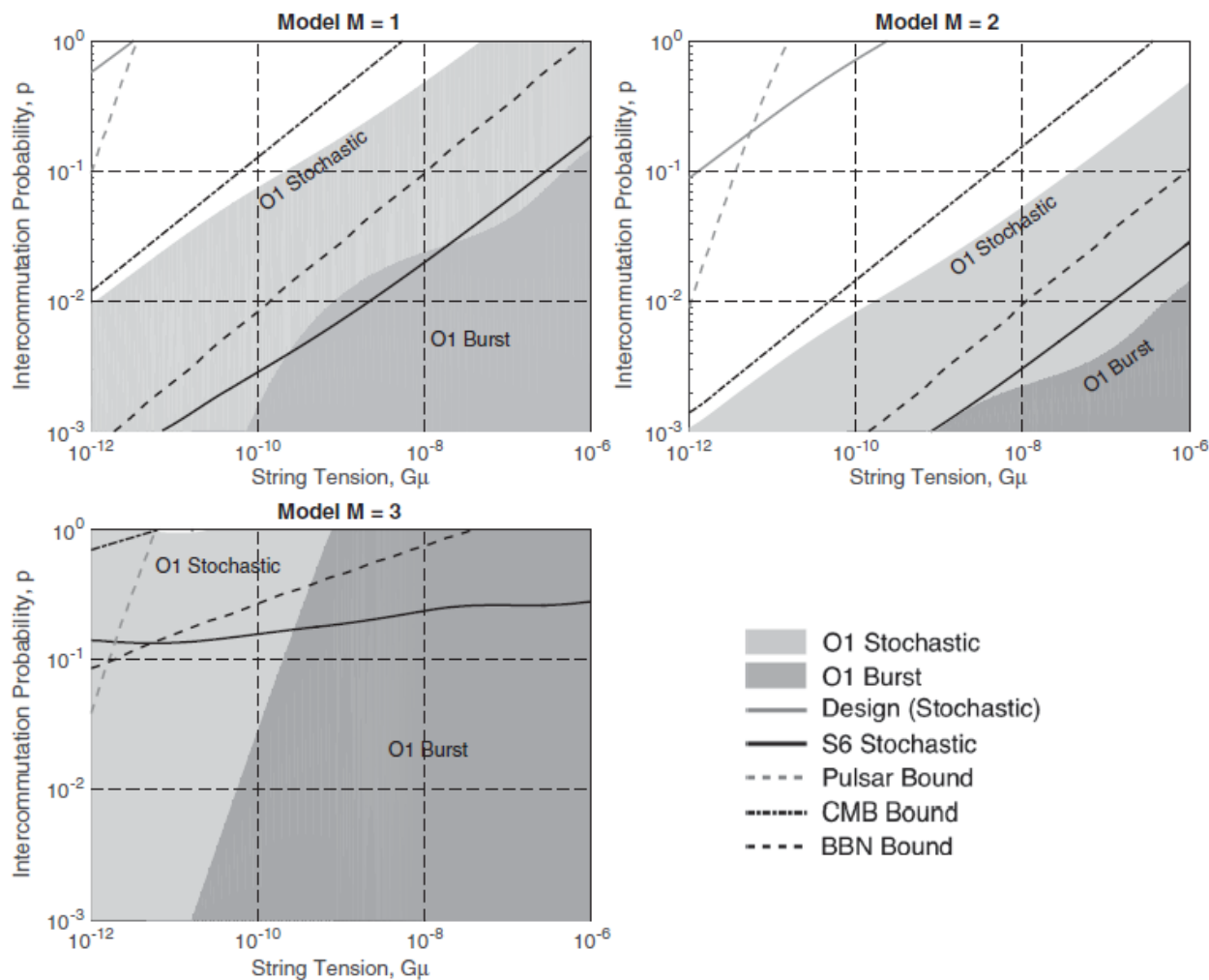
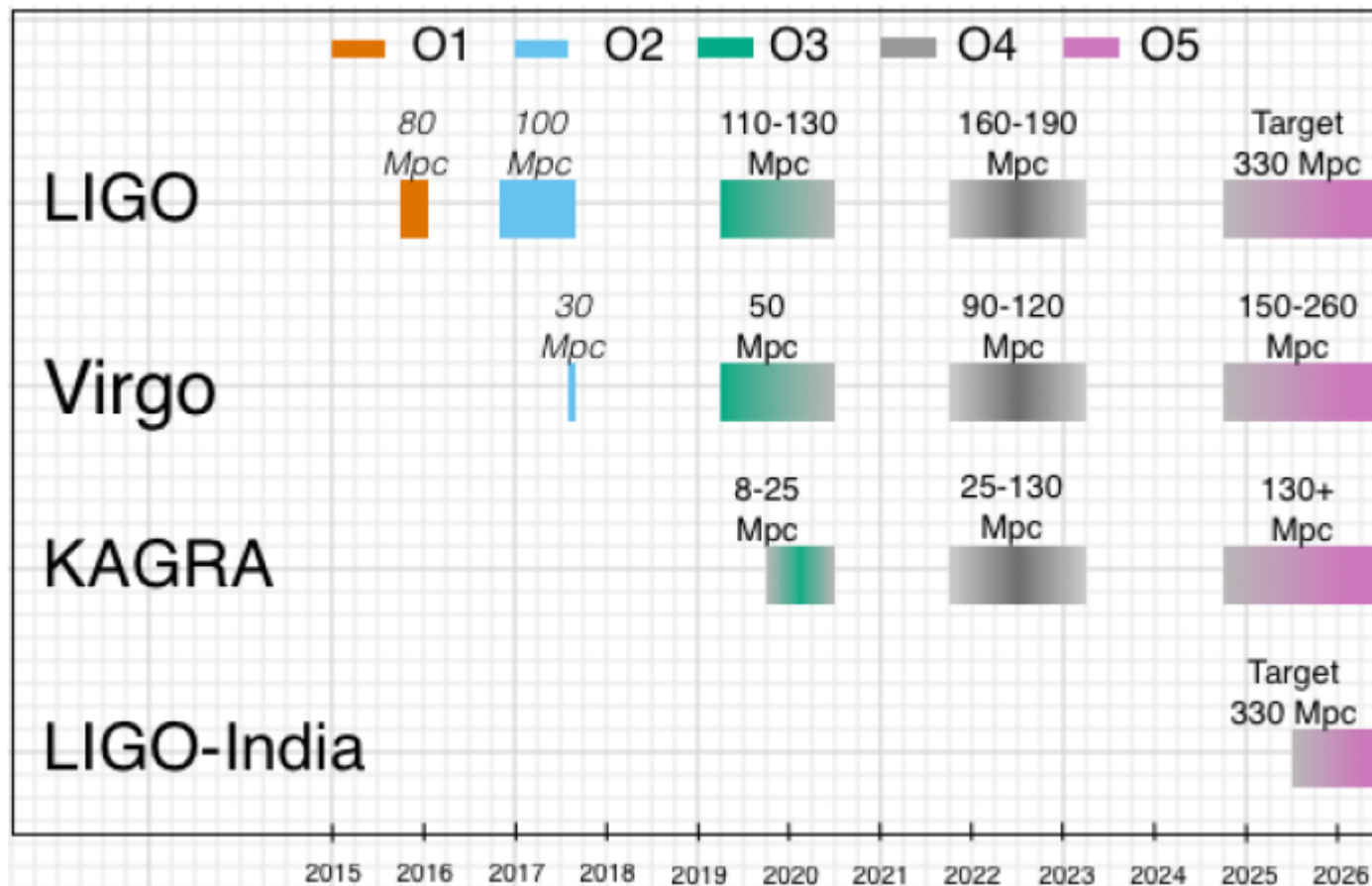


FIG. 6. 95% confidence exclusion regions are shown for three loop distribution models: $M = 1$ (top left), $M = 2$ (top right), and $M = 3$ (bottom left). Shaded regions are excluded by the latest (O1) Advanced LIGO stochastic [31] and burst (presented here) measurements. We also show the bounds from the previous LIGO-Virgo stochastic measurement (S6) [63], from the indirect BBN and CMB bounds [27,28], and from the PTA measurement (pulsar) [29]. Also shown is the projected design sensitivity of the Advanced LIGO and Advanced Virgo experiments (design, stochastic) [64]. The excluded regions are below the respective curves.

Future Observing Runs



The planned sensitivity evolution and observing runs of the aLIGO, AdV and KAGRA detectors over the coming years.

O3 Stochastic Update

- O3 sensitivity better than O2
- O3, 1-year of observation
- Assuming 50% duty cycle, might get a factor of 3 improvement on limit for Ω_{gw}
- Combined O1-O2-O3 analysis, you can do the math: $\Omega_{\text{GW}} \propto 1/\sqrt{T}$
- Sensitivity improvement will have the biggest effect
- Inclusion of Virgo in O3 not likely to change isotropic limit, but will have important implications for the directional searches.
- With Virgo, three detector combinations, and improved sky resolution.

LIGO-Virgo Summary/Conclusion

- The GW stochastic background from BBHs and BNSs is approaching a detectable level
- The background may be measured by LIGO/Virgo operating at or near design sensitivity.
- No evidence for a stochastic background in O1-O2.
- Upper limit on a flat spectrum 2.8 better than for O1
- O3 could see a x 3 improvement on limit for Ω_{gw}